Theoretical predictions of the structural and elastic properties of Mg_2Sr Laves phase under high pressure

DU XIAOMING[a*], CHEN RUIQIANG [a], LIU LINGLING[b]
[a] *School of Materials Science and Engineering, Shenyang Ligong University, Shenyang 110159, China*
[b] *Henan Mechnicial and Electrical Engineering College, Xinxiang 453003 , China*

The structural, elastic and thermodynamic properties and phase stability of Mg_2Sr Laves phase under high pressure have been investigated by means of first-principles method within the framework of density functional theory. The calculated equilibrium structural parameters in present work are in agreement with the available experimental and other theoretical data. The pressure dependence of the elastic constants, polycrystalline elastic moduli, Poisson's ratio, elastic anisotropy, and Vickers hardness of Mg_2Sr are investigated. It is found that the pressure has an important effect on the mechanical properties of Mg_2Sr. Further, the dependences of the Debye temperature and melting temperature on pressure of Mg_2Sr are predicted on the basis of the elastic properties. It is found that the Debye temperature and melting temperature increases with applied pressure. Finally, the density of state and charge density are investigated to understand the bonding characteristics of Mg_2Sr. It is observed that the metallic bonding characteristics becomes stronger with applied pressure.

(Received September 27, 2015; accepted April 05, 2016)

Keywords: Mg_2Sr, Laves phase, Electronic structure, Elastic property, High pressure

1. Introduction

The interest in Magnesium-based alloys is continuously increasing, especially because of their applications in the transportation industry for weight reduction and the consequent increased fuel efficiency [1,2]. However, due to the heat resistance, low strength and ductility, magnesium alloys were limited to the application in many fields. Strontium is an important additive used in magnesium alloys which reduces the shrinkage and porosity of the alloy, and can refine the grains of alloy. Recent experimental investigation indicated that Sr additions could effectively refine the grains of magnesium alloys [3-6], and improve greatly the heat resistance of Mg-Al alloys by forming Al_4Sr, Mg_2Sr and $Mg_{23}Sr_6$ phases [7]. Theoretically, Zhou et al. [8] investigated the electronic, structural and mechanical properties of Mg_2Sr under zero pressure with a exchange-correlation functional in the general gradient approximation. Aljarrah et al. [9] carried out thermodynamic description of the Mg-Ca-Sr system using the modified quasi-chemical model and the Mg-Ca-Sr phase diagram is calculated. The phase stability, elastic and electronic properties of the Mg_2Sr compound were calculated within the framework of density functional theory [10].

Despite substantial efforts in addressing physical properties of Mg_2Sr compound, most of the previous works were performed under the zero pressure. The dependence of structural and mechanical properties of Mg_2Sr Laves phase on pressure has not yet been studied by using the theoretical or experimental method. In this paper, we present a detailed theoretical study of the structural, electronic, mechanical and thermodynamic properties of Mg_2Sr in the pressure of 0 to 40 GPa in the framework of density functional theory (DFT).

2. Computation details

All calculations were performed by using the first principle calculations based on density functional theory [11] implemented in Quantum-ESPRESSO program package [12]. Meanwhile, the exchange and correlation energies were calculated by the generalized gradient approximation (GGA) in the scheme of Perdew-Burke-Eruzerhof (PBE) [13]. The Monkhorst-Pack scheme [14] was used for k point sampling in the first irreducible Brillouin zone (BZ). The k points separation in the Brillouin zone of the reciprocal space was 8×8×6. The kinetic cutoff energy for plane waves was set as 400.0 eV. Pseudo-atom calculations were performed for Mg $2p^6 3s^2$ and Sr $4d^2$ $4p^6$ $5s^2$. The convergence criteria for geometry optimization was as follows: electronic self-consistent field (SCF) tolerance less than 5.0×10^{-5} eV/atom, Hellmann-Feynman force

below 0.01eV/Å, maximum stress less than 0.05GPa and displacement within 2.0×10^{-4} Å. The Brodyden-Fletcher-Goldfarb-Shanno (BFGS) minimization scheme [15] was used to minimize the total energy and internal forces. The elastic constants of Mg_2Sr were obtained by the stress-strain method [16,17].

3. Results and discussion

3.1 Structural properties

Mg_2Sr crystallizes in C14-type Laves phase structure with symmetry $P6_3/mmc$ [18], and the unit cell of Mg_2Sr contains 8 Mg atoms and 4 Sr atoms. Geometry optimization for Mg_2Sr has been performed by full relaxation of cells shape and atomic positions to obtain the equilibrium structural parameters. The equilibrium lattice parameters a, c, and c/a are listed in Table 1, where the available experimental [18] and other theoretical results [10] were also presented. The calculated lattice parameters deviate from the experimental value within 0.3 %. The discrepancy between the experiments and the calculated results can be attributed to the effect of temperature. By fitting the third-order Birch-Murnaghan equation of state (EOS) [19]:

$$P(V)=\frac{3B_0}{2}\left[\left(\frac{V_0}{V}\right)^{\frac{7}{3}}-\left(\frac{V_0}{V}\right)^{\frac{5}{3}}\right]\times\left\{1+\frac{3}{4}(B_0'-4)\left[\left(\frac{V_0}{V}\right)^{\frac{2}{3}}-1\right]\right\} \quad (1)$$

where P is pressure, B_0 and $B'_0$is the bulk modulus at zero pressure and pressure derivative, respectively. V_0 is unit cell volume at zero pressure. The bulk modulus B_0 at zero pressure and its pressure derivative B'_0 of Mg_2Sr are obtained to be 21.061 GPa and 3.762, respectively, as shown in Table 1.

Table 1. Calculated cell parameters, bulk modulus B_0, and its pressure derivative B'_0 of Mg_2Sr at zero pressure, compared with the available experimental and other theoretical values.

	a_0 (Å)	c_0 (Å)	c_0/a_0	V_0 (Å^3)	B_0 (GPa)	B'_0
This work	6.457	10.422	1.614	376.308	21.061	3.762
Cal.[10]	6.468	10.466	1.618	379.073	25.759	3.607
Exp.[18]	6.475	10.430	1.611	378.70	-	-

To investigate the response of Mg_2Sr to the external pressure, the relative changes of lattice parameters a and c with increasing pressure are presented in Fig. 1. It is found that the a/a_0 and c/c_0 decreases smoothly with the applied pressure, where a_0 and c_0 is the equilibrium lattice parameters at zero pressure, respectively. The acquired relations can be expressed as:

$$a/a_0=0.998-0.0073P+7.76\times10^{-5}P^2 \quad (2)$$

$$c/c_0=0.994-0.0075P+8.71\times10^{-5}P^2 \quad (3)$$

Moreover, Fig.1 also shows the relative change of unit cell volume V/V_0 as a function of the external pressure. As the pressure increases, the distance between atoms becomes smaller due to the mutual repulsion of the atoms, which leads to the difficulty of compression in Mg_2Sr crystal under compression. Thus, it can be found that the curves of a/a_0, c/c_0 and V/V_0 become more moderate with increasing pressure. It also indicates that there is no phase transition for Mg_2Sr according to the smooth variations of a/a_0, c/c_0 and V/V_0.

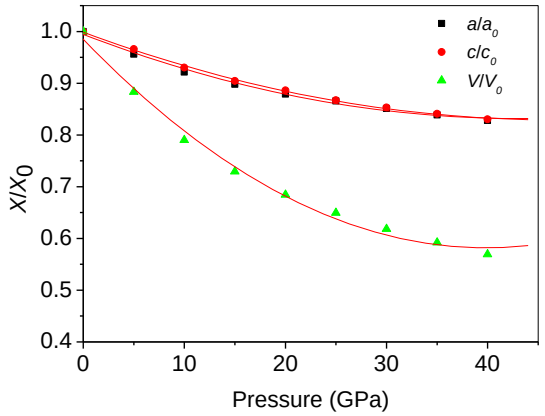

Fig. 1. The normalized lattice parameters ($a/a_0$and c/c_0) and volume V/V_0 as a function of pressure ranges from 0 to 40 GPa for Mg_2Sr at 0 K.

3.2 Elastic properties

Elastic constants are the measure of the resistance of a crystal to an externally applied stress. Through imposing small strain on the perfect lattice, the elastic constants can be obtained. For hexagonal Mg_2Sr crystal, there are only

five independent elastic constants, i.e., C_{11}, C_{12}, C_{13}, C_{33}, and C_{44}, since $C_{66} = (C_{11} - C_{12})/2$. The calculated elastic constants at the ground states together with the available theoretical data [8, 20] are listed in Table 2. The calculated elastic constants of Mg_2Sr are good agreement with the available reported data. The intrinsic mechanical stability of a solid is in general determined by certain conditions related to the crystal symmetry. The mechanical stabilities of Mg_2Sr has been analyzed according to elastic constants. For hexagonal crystal, the elastic constants need to satisfy the mechanical stability criterion [21]:

$$\begin{aligned} &C_{11} > 0, C_{11} - |C_{12}| > 0 \\ &C_{44} > 0, (C_{11} + C_{12})C_{33} - 2C_{13}^2 > 0 \end{aligned} \quad (4)$$

From Table 2, it is obvious that the calculated elastic constants satisfy the mechanical stability criterion. This implies that Mg_2Sr is mechanically stable at pressure below 40 GPa. It can be seen that the C_{11} and C_{33} are much larger than the other elastic constants, which indicates that Mg_2Sr is incompressible under uniaxial stress along *a* or *c* axis.

Table 2. The calculated elastic constants C_{ij} (in GPa) of Mg_2Sr at zero pressure in comparison with available values.

	C_{11}	C_{12}	C_{13}	C_{33}	C_{44}
This work	35.68	9.99	10.49	57.87	13.76
Cal.[20]	43.80	19.80	10.60	57.20	12.40
Cal.[8]	48.40	22.67	12.46	57.96	13.15

Additionally, Fig. 2 (a) shows the variations of the elastic constants of Mg_2Sr under different pressures. It can be found that the five independent elastic constants increase monotonically with increasing pressure. It is indicated that bonding strength is enhanced by applying external pressure. The C_{11} and C_{33} are more sensitive to the change of pressure than C_{12} and C_{13}. This can be explained by the differences of the compressibility at different directions. It is well known that the C_{44} is the most significant parameter which is associated with deformation resistance to shear in the (100) plane. It can be seen from Fig. 2 (a) that the C_{44} increases comparatively slowly with increasing pressure, which indicates that the external pressure has little influence on the shear deformation resistance.

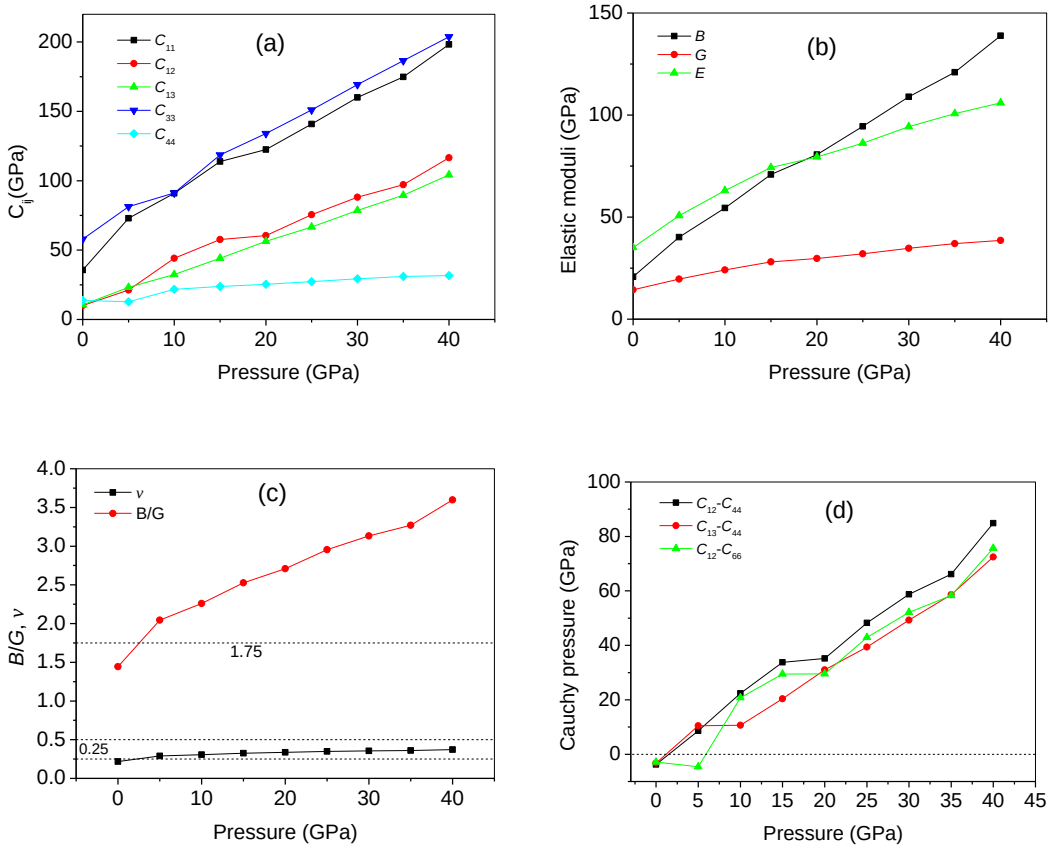

Fig.2. The pressure dependence of the elastic properties for Mg_2Sr, (a) elastic constants, (b) elastic.

Moduli, (c) *B/G* and Poisson's ratio *v* and (d) Cauchy pressure.

The elastic properties of polycrystalline materials are usually characterized by the elastic moduli, such as bulk modulus (*B*), Young's modulus (*E*), shear modulus (*G*) and Poisson ratio ν. On the basis of the approximations by Voigt [22] and Reuss [23] and Hill's empirical average[24], we have calculated the corresponding bulk moduli $B=(B_V+B_R)/2$, shear moduli $G=(G_V+G_R)/2$ (where the subscripts V and R refer to the Vigot and Reuss bounds, respectively.), Young's modulus *E* and Poisson ratio ν under different pressure. The Young's modulus *E* and Poisson ratio ν can be expressed as the following formula [25]:

$$E = 9BG/(3B+G) \tag{5}$$

and

$$\nu = (3B-2G)/(6B+2G) \tag{6}$$

The calculated results are shown in Table 3 (along with other theoretical values [8,20]) and Fig. 2 (b) and Fig. 2 (c). Form Fig. 2 (b) it can be found that the calculated elastic modulis (*B*, *G* and *E*) increase with applied pressure, which is similar to the trend of elastic constants. On the other hand, Poisson's ratio ν is used to quantify the stability of the crystal against shear, which can provide more information on the characterizations of the bonding forces than elastic constants [26]. The ν with a value of 0.25 and 0.5 is the lower limit and upper limit for central force solids, respectively [27]. In this work, the calculated value of ν at zero pressure less than the lower limit 0.25, as listed in Table 3, which indicates that Mg_2Sr crystal is with minor central inter-atomic forces. Moreover, The ratio of the bulk modulus *B* to shear modulus *G* of the compounds, proposed by Pugh [28], can empirically predict the brittle and ductile behavior of materials. The compound with smaller *B/G* ratio (<1.75) usually is brittle while the compound with larger *B/G* ratio (>1.75) is ductile. Table 3 and Fig. 2 (c) show the effect of pressure on the *B/G* ratio of Mg_2Sr. It is found that the *B/G* ratio of Mg_2Sr increases with applied pressure. Particularly wish to point out that the *B/G* ratio at zero pressure is smaller than 1.75, then the values larger than 1.75 appear above 2 GPa. It indicates that the pressure will have an important effect on the ductility of Mg_2Sr, and favors the ductility of Mg_2Sr above 2 GPa.

Table 3. The calculated bulk modulus B (GPa), shear modulus G (GPa), Young's modulus E (GPa), B/G, Poisson's ratio v and Vickers hardness H_v for Mg_2Sr.

Pressure	*B*	*G*	*E*	*B/G*	*v*	H_v
0	20.8	14.4	35.1	1.444	0.219	3.19
	31.26[a]	13.04[a]	34.35[a]	2.398[a]	0.317[a]	
	25.2[b]	13.8[b]	36.1[b]	1.818[b]	0.26[b]	
5	40.2	19.7	50.7	2.045	0.289	1.96
10	54.5	24.1	63.0	2.261	0.307	1.94
15	70.9	28.0	74.3	2.527	0.325	1.75
20	80.6	29.7	79.4	2.709	0.336	1.53
25	94.5	32.0	86.2	2.954	0.348	1.28
30	108.9	34.8	94.3	3.133	0.356	1.19
35	120.9	37.0	100.7	3.270	0.361	1.13
40	138.9	38.6	106.0	3.598	0.373	0.79

[a] Ref. [8]
[b] Ref. [20]

One of the Cauchy pressure components, C_{12}-C_{44} can be also used to described the brittle and ductile behavior of materials [29]. The critical value which separates ductile and brittle material is about zero. The material behaves in a ductile manner if C_{12}-C_{44}>0, otherwise brittle manner. The calculated values of C_{12}-C_{44} for Mg_2Sr are shown in Fig. 2 (d). It is found that the C_{12}-C_{44} at zero pressure is smaller than zero, then the positive values appear with the increase of pressure. This change under the influence of pressure is same as the *B*/*G* ratio. Other two Cauchy pressure components, C_{13}-C_{44} and C_{12}-C_{66} can predict the bonding behaves of materials [30]. If the values of C_{13}-C_{44} and C_{12}-C_{66} are positive, the materials show metallic bonds, otherwise covalent bonds. The larger the values are, the stronger the metallic properity is. The calculated values of C_{13}-C_{44} and C_{12}-C_{66} for Mg_2Sr show that the metallic property is predominant above 5 GPa, as shown in Fig.2 (d), and becomes stronger with applied pressure.

The hardness of a material is one of a very important mechanical properties in materials design. The theoretical Vickers hardness of Mg_2Sr was calculated by the following relation [31]:

$$H_v = 2(\lambda^2 G)^{0.585} - 3 \tag{7}$$

where $\lambda = G/B$ is Pugh's modulus ratio. The calculated Vickers hardness of Mg_2Sr under different pressures is shown in Table 3. It can be seen that the Vickers hardness decreases monotonically with the increasing pressure which suggests that the pressure is unfavourable to the hardness of Mg_2Sr.

3.3 Elastic anisotropy

The elastic constants of solids are very important because they are closely associated with the mechanical and physical properties. In particular, they play an important part in providing valuable information about structural stability and anisotropic characteristics.

The universal elastic anisotropy index A^U for crystals with any symmetry is proposed as follow [32]:

$$A^U = 5\frac{G_V}{G_R} + \frac{B_V}{B_R} - 6 \geq 0 \tag{8}$$

where B_V (G_V) and B_R (G_R) are the bulk modulus (shear modulus) in the Voigt and Reuss approximations. A crystal with $A^U = 0$ means it is isotropic. The deviation of A^U from zero defines the extent of single crystal anisotropy (i. e. the larger A^U represents the more anisotropic) and accounts for both the shear and the bulk contributions unlike all other existing anisotropy measures. Obviously, the increase in the G_V/G_R affects the anisotropy A^U much more than in B_V/B_R because of the coefficient for G_V/G_R (=5) larger than that for B_V/B_R (=1). The calculated values of A^U for Mg_2Sr under various pressure are listed in Table 4. The A^U of Mg_2Sr at zero pressure is 0.219, which indicates that the Mg_2Sr exhibits a little anisotropic elasticity. A maximum appears at 5 GPa, then the A^U keeps small oscillations as the pressure increases. It means that the pressure will have an important effect on the elastic anisotropy of Mg_2Sr.

To distinguish the shear and the bulk contributions to elastic anisotropy of Mg_2Sr, the elastic anisotropy in compressibility and shear is expressed using two dimensionless quantities, respectively [33]:

$$A_B = \frac{B_V - B_R}{B_V + B_R} \tag{9}$$

$$A_G = \frac{G_V - G_R}{G_V + G_R} \tag{10}$$

The value of zero represents elastic isotropy and the value of unity indicates the largest possible anisotropy. The calculated values of A_B and A_G are listed in Table 4. It is found that the values of A_B at zero pressure is 0.023, which indicates that the Mg_2Sr exhibits a little anisotropic elasticity in compressibility. The value of A_B is colse zero above 5 GPa, which is approximately isotropic in compressibility. The variation trends of A_G are similar to A^U, which indicates the elastic anisotropy in shear is predominant for Mg_2Sr.

Table 4. Calculated elastic anisotropic parameters under various pressure of Mg_2Sr.

Pressure	A^U	A_B	A_G	B_a, GPa	B_c, GPa	$1/\beta$
0	0.219	0.023	0.017	51.1	98.1	1.919
5	0.676	0.002	0.063	113.3	137.6	1.214
10	0.097	0.001	0.009	173.9	145.4	0.836
15	0.161	0	0.016	220.7	197.9	0.897
20	0.111	0	0.011	234.0	258.5	1.104
25	0.125	0	0.012	282.1	286.4	1.015
30	0.131	0	0.013	327.0	326.2	0.998
35	0.135	0	0.013	357.7	373.5	1.044
40	0.164	0	0.016	426.3	398.4	0.934

we also considered the anisotropy in linear bulk modulus. For hcp crystal, the linear bulk modulus along the a- and c-axes, B_a and B_c can be defined as follows [34]:

$$B_a = a\frac{dp}{da} = \frac{\Lambda}{2+\beta} \tag{11}$$

$$B_c = c\frac{dp}{dc} = \frac{B_a}{\beta} \tag{12}$$

where

$$\Lambda = 2(C_{11} + C_{12}) + 4C_{13} + C_{33}\beta^2 \tag{13}$$

$$\beta = \frac{C_{33} - C_{13}}{C_{11} + C_{12} - 2C_{13}} \tag{14}$$

The value of unity for $1/\beta$ represents the elastic isotropy in compressibility, otherwise elastic anisotropy in compressibility. The calculated values of B_a, B_c and $1/\beta$ are listed in Table 4. The results showed that the bulk modulus

B_a and B_c of Mg_2Sr under variuos pressure is different, indicating that the Mg_2Sr deviated from isotropy. The $1/\beta$ of Mg_2Sr at zero pressure is 1.919, which indicates that the Mg_2Sr exhibits a obvious anisotropic elasticity. When the pressure is increased to 25 GPa, Mg_2Sr is approximately isotropic for elasticity. This result suggests that the elastic anisotropy of Mg_2Sr Laves phase is dependent on the external pressure.

3.4 Thermodynamic properties

The Debye temperature θ_D is a fundamental attribute of a solid connecting elastic properties with thermodynamic properties such as specific heat, sound velocity and melting temperature. It can be calculated from the averaged sound velocity, v_m by the following equation [35]:

$$\theta_D = \frac{h}{k_B}\left[\frac{3n}{4\pi}\left(\frac{N_A\rho}{M}\right)\right]^{\frac{1}{3}} v_m \quad (15)$$

where h is Planck's constant, k_B is Boltzmann's constant, N_A is Avogadro's number, n is the number of atoms in the unit cell, M is the molecular weight and ρ is the density. The average sound velocity in the polycrystalline material is approximately given by [35]:

$$v_m = \left[\frac{1}{3}\left(\frac{2}{v_s^3} + \frac{1}{v_l^3}\right)\right]^{-1/3} \quad (16)$$

where v_l and v_s are the longitudinal and transverse sound velocity, respectively, which can be obtained using the shear modulus G and the bulk modulus B from Navier's equations [36]:

$$v_l = \sqrt{\frac{B + 4G/3}{\rho}} \quad \text{and} \quad v_s = \sqrt{\frac{G}{\rho}} \quad (17)$$

The calculated θ_D with a step of 5 GPa from 0 GPa to 40 GPa are listed in Table 5. The Debye temperature obtained here is 247.6 K at 0 GPa, which agrees well the theoretical value of 278.0 K [10]. To our knowledge, there are no existing experimental values of Debye temperature for Mg_2Sr. So the comparison between the value in this work and the experimental values cannot be made. As shown in Table 5, it can be seen that Debye temperature increases with applied pressure. It is indicated that the strength of covalent bonds for Mg_2Sr Laves phase increases with increase of pressure.

Table 5. The calculated density (ρ), the longitudinal, transverse, and average sound velocity (v_l, v_s, v_m), the Debye temperatures (θ_D).

Pressure	v_l (m·s^{-1})	v_s(m·s^{-1})	v_m(m·s^{-1})	ρ (kg·m^{-3})	θ_D (K)	T_m (K)
0	3233	2444	2621	2407	247.6	776.8
5	3553	2686	2881	2724	283.6	907.6
10	3721	2813	3017	3045	308.2	975.5
15	3858	2916	3127	3298	328.1	1061.7
20	3847	2908	3119	3515	334.2	1106.0
25	3888	2939	3152	3703	343.7	1176.6
30	3954	2989	3205	3892	355.3	1252.2
35	3991	3017	3235	4065	363.9	1312.8
40	3999	3023	3242	4225	369.3	1405.2

The melting temperature is considered to be an important index to evaluate heat resistance of alloy materials. For hexagonal structural metals, the melting temperature, T_m can be expressed as [37]:

$$T_m = 354\,\text{K} + (4.50\,\text{K/GPa})C_{11} + 2C_{33} \pm \quad (18)$$

In present work, a minus sign can be slected in the Eq. (17). The calculated values of the melting temperature for Mg_2Sr are listed in Table 5. It can be seen that the melting temperature increases with the increasing of pressure. As a result, the heat resistance of Mg_2Sr phase can be improved by the applied pressure correspondingly.

3.5 Electronic structure

The effect of pressure on the electronic structure of Mg_2Sr has been also studied. The equilibrium density of states (DOS) and the pressure dependence of DOS are shown in Fig. 3, in which the Fermi level is set to zero. The most remarkable feature of the total DOS (TDOS) under variuos pressure is that the values of the TDOS at Fermi level is larger than zero, which indicated all the phases exhibit metallic character. The obtained metallic character is consistent with the general characteristic of Laves phases [38]. The bonding electron numbers at the Fermi level ($N(E_F)$) is 0.816, 0.685, 0.651 and 0.595 electron /eV/atom for Mg_2Sr at 0, 10, 20, and 40 GPa, respectively, which are mainly contributed by electrons from Mg 3s and Sr 4d with small contribution of Mg 2p and Sr 5s orbits. In general, $N(E_F)$ on DOS plot can be used to characterize the activity of valance electrons of the atoms in crystal. Namely, the smaller $N(E_F)$, the less is change probability of the electronic structures of the crystal when external conditions change, thus the crystal

has the higher stability [39]. It is found that the $N(E_F)$ decreases by about 27 % from 0 GPa to 40 GPa, which indicates that the applied pressure is beneficial to the stability of Mg_2Sr.

In Fig. 3, we can see that the main bonding peaks for Mg_2Sr under various pressure basically locate in energy range from 4 to -6 eV, and mainly originate from the contribution of valance electron numbers of Mg 3s, Mg 2p, Sr 5s, and Sr 4d orbits and basically the contribution of Sr 4p orbit can be neglected. The TDOS of Mg_2Sr near the Fermi level is mainly originated from Mg 2p and Sr 4d with small contribution of Mg 3s and Sr 5s orbits. The shapes of the peaks of TDOS under various pressure show slight changes, which indicates that Mg_2Sr is still structural stable and there is no phase transformation under the pressure up to 40 GPa. Interestingly, the TDOS shows the presence of the pseudogap near the Fermi level at 0 GPa, as shown in Fig. 3(a). This illustrates that there exists a strong hybridization effect in Mg_2Sr crystal in equilibrium state. From Fig. 3 (a), it can be seen that the Mg 3s orbit hybridize strongly with the Sr 4d orbit above the Fermi level, implying that the covalent bonds exist in the Mg_2Sr crystal. Besides, the hybridization exists between the 3s and 2p orbits of Mg atoms and 5s and 4d orbits of Sr atoms among the valence band. As the pressure increases, the hybridization between the 3s and 2p orbits of Mg atoms and 5s and 4d orbits of Sr atoms above the Fermi level becomes weaker, as shown in Fig. 3 (b)-(d), implying that the metallic property of Mg_2Sr crystal becomes stronger. This result may be explained by ordering of the electrons in the conduction band with the applied pressure. Below the Fermi level, the bonding peaks in TDOS and partial DOS (PDOS) of Mg and Sr atoms become wider with increasing pressure. These results may be explained by the variations of the spacing between atoms as well as the overlap of wave functions under compression. The intensity of the bonding peaks in TDOS and PDOS gradually decreases with applied pressure, implying the hybridization between the 2p orbits of Mg atoms and 4d orbits of Sr atoms becomes weak. Beside, the shifting of the bonding peaks towards the low energy region and the antibonding peaks towards the high energy region can be observed in TDOS and PDOS with applied pressure. These phenomena can be explained by the delocalization among the bonding atoms in Mg_2Sr crystal.

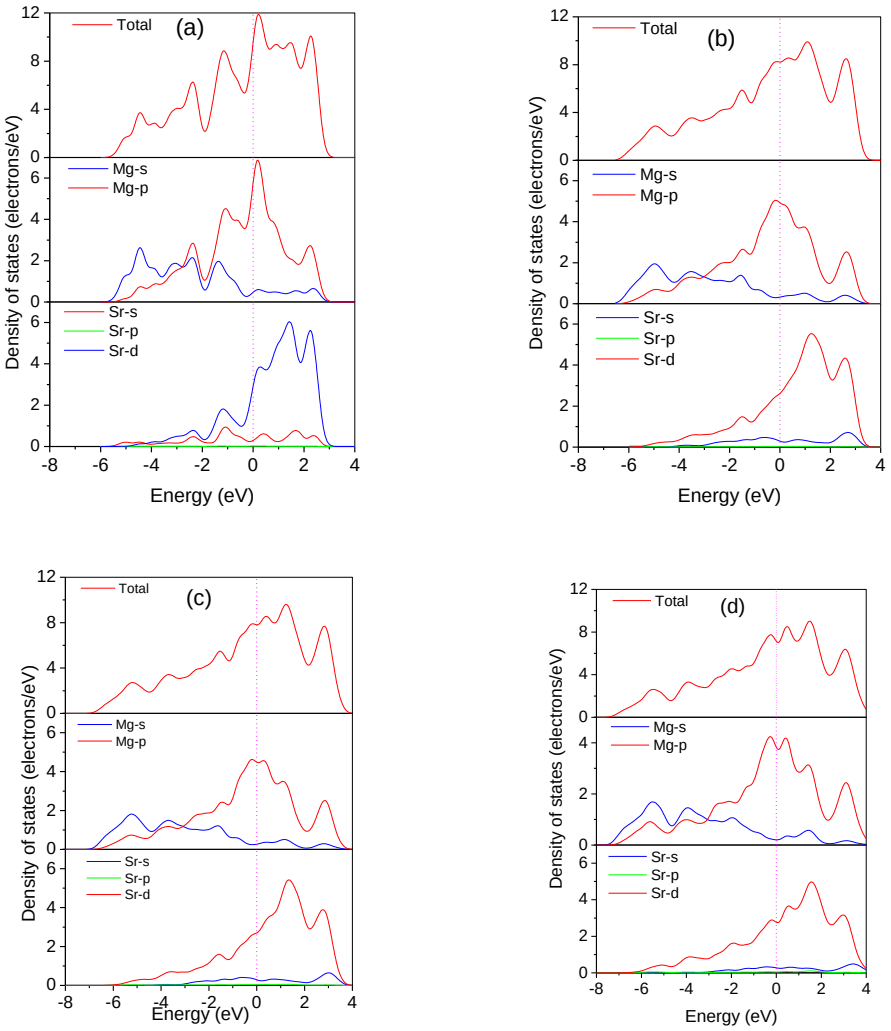

Fig. 3 The partial and total DOS of Mg_2Sr at 0 GPa (a), 10 GPa (b), 20 GPa (c)and 40 GPa (d). The vertical dotted lines represent the Fermi level.

To visualize the nature of the bond character and to explain the charge transfer and the bonding properties of the Mg_2Sr under various pressure, we have investigated change of the charge density (e/Å^3) distribution. Fig. 4 shows the charge-density contour on the (110) plane at 0, 10, 20, and 40 GPa for Mg_2Sr. From Fig. 4, it is found that the bonding between Sr and its adjacent Sr atom is mainly covalent, the bonding between Sr and Mg is ionic and the bonding between Mg and Mg is metallic. As the pressure increases, the absolute value of the charge density around atoms also increase. However, the charge density between Mg and Mg atom increases more rapidly than that of Mg and Sr atom, Sr and Sr atom which means that the metallic property under high pressure becomes stronger than that under 0 GPa. The bonding characteristics of Mg_2Sr are a combination of metallic, covalent, and ionic nature.

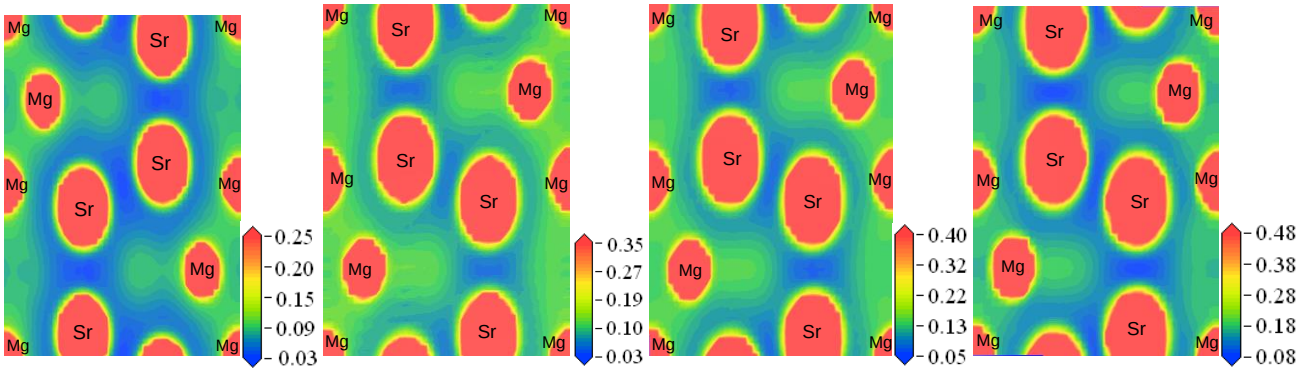

(a) *(b)* *(c)* *(d)*

Fig. 4. Charge density plot of Mg_2Sr in the (110) plane, (a) 0 GPa, (b) 10GPa, (c) 20 GPa, (d) 40GPa, the unit of scale is e·Å^{-3}.

4. Conclusions

In present work, the structural, mechanical, electronic and thermodynamic properties of Mg_2Sr Laves phase under pressure range from 0 to 40 GPa have been investigated by using the first-principle calculations in the framework of density functional theory. It is found that the calculated structure parameters at 0GPa are consistent with the previous experimental and theoretical data. There is no phase transformation for Mg_2Sr Laves phase under the pressure up to 40 GPa. The elastic constants, polycrystalline elastic moduli, Poisson's ratio, elastic anisotropy and Vickers hardness of Mg_2Sr determined by using the Voigt–Reusse–Hill approximation at various pressures are successfully calculated. It is found that the pressure has an important effect on the mechanical properties of Mg_2Sr. Additionally, the dependences of the Debye temperature and melting temperature on pressure of Mg_2Sr are obtained. It is found that the Debye temperature and melting temperature increases with applied pressure. Finally, the DOS and charge density distribution under high pressure have been analyzed in order to explain the bonding characteristics of the Mg_2Sr. The bonding characteristics of Mg_2Sr is a combination of metallic, covalent, and ionic nature, and the metallic property of Mg_2Sr crystal becomes stronger with the increase of pressure.

References

[1] R. Gradinger, P. Stolfig, Proc. Mine. Metals Mater. Soc. (TMS), p. 231, 2003.
[2] S. Das, JOM, **55**, 22 (2003).
[3] A. Srinivasan, U. T. pillai, J. Swaminathan, S. K. Das, B. C. Pai, J. Mater. Sci., **41**, 6087 (2006).
[4] K. Y. Nam, D. H. Song, C. W. Lee, Mater. Sci. Form, **510/511**, 238 (2006).
[5] H. Kinji, S. Hidetoshi, T. Yorinobu, Mater. Sci. Eng. A, **403**, 276 (2005).
[6] Yang M. B., Pan F. S., Cheng R. J., Tang A. T., Trans Nonferrous Met. Soc. China, **18**, 52 (2008).
[7] Zhong Y., J. O. Sofo, Luo A. A., Liu Z. K., J. Alloy Compd., **421**, 172 (2006).
[8] Zhou D., Liu J., Peng P., Trans. Nonferrous Met. Soc. China, **21**, 2677 (2011).
[9] M. Aljarrah, M. Medraj, Computer Coupling of Phase Diagrams and Thermochemistry, **32**, 240 (2008).
[10] Mao, P., Yu B., Liu Z, Feng W., Yang J, J. Appl. Phys. **117**, 115903 (2015).
[11] W. Kohn, L. J. Sham, Phys. Rev. A. **140**, 1133 (1965).
[12] http://www.pwscf.org.
[13] J. P. Perdew, K. Burke, M. Ernzerhof, Phys. Rev. Lett. **77**, 3865 (1996)
[14] H. J. Monkhorst, J. D. Pack, Phys. Rev. B **13**, 5188 (1976).
[15] T. H. Fischer, J. Almlof, J. Phys. Chem. **96**, 9768 (1992).
[16] J. Feng, B. Xiao, R. Zhou, W. Pan, D.R. Clarke, Acta Mater. **60**, 3380 (2012).
[17] V. Miman, M. C. Warren, J. Phys. Condens. Matter. **13**, 241 (2001).
[18] M. M. Makhmudov, O. I. Bodak, A. V. Vakhobov, T. D. Dzhurayev, Russ. Metall., **6**, 209 (1981).
[19] F. Birch, J. Geophys. Res. **83**, 1257 (1978).
[20] Z. Yang, J. Du, B. Wen, Ch. Hu, R. Melnik, Intermetallics, **32**, 156 (2013).
[21] J. F. Nye, Physical Properties of Crystals (Clarendon

Press, Oxford, 1964).
[22] W. Voigt, Lehrbuch der Kristallphysik, Teubner, Leipzig, 1928.
[23] A. Reuss, Z. Angew. Math. Mech. **9**, 49 (1929).
[24] R. Hill, Proc. Phys. Soc. London **65**, 349 (1952).
[25] A. M. Hao, X. C. Yang, X. M. Wang, Y. Zhu, X. Liu, R. P. Liu, J. Appl. Phys., **108**, 063531 (2010).
[26] B. Mayer, H. Anton, E. Bott, M. Methfessel, J. Sticht, P.C. Schmidt, Intermetallics **11**, 23 (2003).
[27] H. Z. Fu, D. H. Li, F. Peng, T. Gao, X. L. Cheng, Comput. Mater. Sci. **44**, 774 (2008).
[28] S. F. Pugh, Phil. Mag., **45**, 823 (1954).
[29] D. G. Pettifor, Mater. Sci. Technol. 8, 345 (1992).
[30] S. X. Cui, W. X. Feng, H. Q. Hu, G. Q. Zhang, Z. T. Lv, Z. Z. Gong, J. Solid State Chem. **184**, 786 (2011).
[31] X. Q. Chen, H. Y. Niu, D. Z. Li, Y. Y. Li, Intermetallics **19**, 1275 (2011)
[32] S. I. Ranganathan, M. Ostoja-Starzewski, Phys. Rev. Lett. **101**, 055504 (2008).
[33] D. H. Chung, W. R. Buessem, in: F.W. Vahldiek, S.A. Mersol (Eds.), Anisotropy in Single Crystal Refractory Compound, vol. 2 (Plenum, New York, 1968) 217.
[34] P. Ravindran, L. Fast, P. A. Korzhavyi, B. Johansson, J. Wills, O. Eriksson, J. Appl. Phys., **84** (1998) 4891.
[35] O. L. Anderson, J. Phys. Chem. Solids, **24**, 909 (1963).
[36] E. Schreiber, O. L. Anderson, N. Soga, Elastic constants and their measurements (McGraw-Hill, New York, 1973).
[37] M. E. Fine, L. D. Brown, and H. L. Marcus, Scr. Metall., **18**, 951 (1984).
[38] P. M. Robinson, M. B. Bever, in Intermetallic Compounds, ed. By J.H. Westbrook (Wiley, New York, 1967).
[39] Y. Imai, M. Mukaida, T. Tsunoda, Intermetallics, **8**, 381 (2000)

*Corresponding author: du511@163.com